

Received December 4, 2019, accepted January 3, 2020, date of publication January 13, 2020, date of current version January 22, 2020.

Digital Object Identifier 10.1109/ACCESS.2020.2966270

Energy-Efficient and QoS-Aware Link Adaptation With Resource Allocation for Periodical Monitoring Traffic in SmartBANs

JAUME RAMIS-BIBILONI¹ (Member, IEEE), AND LOREN CARRASCO-MARTORELL¹

Mobile Communications Group, Department of Mathematics and Computer Science, University of the Balearic Islands, 07122 Palma, Spain

Corresponding author: Jaume Ramis-Bibiloni (jaume.ramis@uib.es)

This work was supported by the MINECO (AEI/FEDER, UE), Spain, under Project TERESA-TEC2017-90093-C3-1/2/3-R.

ABSTRACT Limited energy resources of sensors and stringent *quality-of-service* (QoS) constraints in biomedical applications raise serious concerns when utilized in Wireless Body Area Networks (WBANs). The European Telecommunications Standards Institute (ETSI) Smart Body Area Network (SmartBAN) represents a standardized communication interface and protocol between a hub coordinator and a set of sensors, that has been designed with simplicity and low power in mind. This work presents an ETSI SmartBAN PHY and MAC configuration framework that remarkably lengthens sensors battery lifespan through reducing transceivers consumed energy. To that end, and taking into account the channel quality and packet error rate requisites of sensors, a mechanism to select between the different PHY transmission modes of the standard is proposed. This link adaptation scheme is combined with a resource allocation algorithm that derives the duration of the inter-beacon intervals and the transmission periods of sensors, while fulfilling traffic delay constraints and minimizing sensors transceivers energy consumption. Analytical expressions for packet error rate of all available PHY transmission modes, as well as for traffic delay, transceivers energy savings of hub and sensor nodes, and battery duration, are derived. Computer simulation results substantiate the efficacy of both, the presented QoS-aware adaptive transmission scheme and the resource allocation algorithm, in fulfilling the target packet error rate and delay requirements, while significantly expanding the battery duration, specially for sensors with long elapsed times between successive sensing intervals (up to a 515% increase and a 960% increase are obtained for the two considered simulation scenarios).

INDEX TERMS eHealth, ETSI SmartBAN, link adaptation, resource allocation, wireless body area network (WBAN).

I. INTRODUCTION

Wireless body area networks (WBANs) consist of a set of small low power wireless sensors that can be inserted into the body or worn on the skin surface, which communicate the measured data to a hub coordinator. This is expected to be a breakthrough technology in healthcare areas, telemedicine, and physical rehabilitation, supporting the more autonomous, proactive and predictive health-care services required in the near future. But one of the keys to its widespread use is the requisite of low power sensors with a long battery duration. As a result, the *physical* (PHY) and *medium access control* (MAC) layers in emerging WBANs ought to consider the different strategies used by sensors to

reduce energy consumption. As a result, the two standards that have appeared for WBANs, the Institute of Electrical and Electronics Engineers (IEEE) 802.15.6 (2012) [1] and the European Telecommunications Standards Institute (ETSI) Smart Body Area Network (SmartBAN) (2015) [2], [3], include mechanisms to increase the sensors battery lifetime. Nevertheless, the IEEE 802.15.6 complexity hinders a straightforward implementation and assessment of the standard. Contrarily, the ETSI SmartBAN prioritizes simplicity. Comparative analyses [4], [5] demonstrate that ETSI SmartBAN connection times and energy consumption are lower than those obtained with the IEEE 802.15.6 standard. These promising results have inspired to further investigate the capabilities of this new standard in the present paper.

The MAC layer specifications can significantly influence the energy consumption of a sensor network. Energy savings

The associate editor coordinating the review of this manuscript and approving it for publication was Gerhard P. Hancke¹.

can be increased by MAC protocols that switch off the radio when transmission or reception of data is not required [6]. To that end, sensor data can be collected and organized into packets that are periodically transmitted. Notwithstanding the vast majority of WBAN traffic corresponds to periodic uplink transmissions, just a few works analyze scheduled access in WBANs [5], [7]–[10] and even less have investigated periodic traffic performance in the SmartBAN standard [5]. The works in [8]–[10] present MAC protocols for BAN networks with a star configuration that do not conform to any existing standard. The authors in [7] adapt the sensors transmission rate and transmission power in order to minimize the energy consumption while maintaining a set of *quality-of-service* (QoS) constraints. This approach, which considers the channel status and traffic requirements, involves the resolution of an optimization problem that adds a significant amount of complexity to the hub. Moreover, its complete centralization implies an additional delay that hampers its capacity to adapt to channel variations in most environments. In contrast, in this proposal, presented in the following Sections, part of the decision concerning the transmission parameters is performed on the sensors, allowing a faster response to channel changes. Another centralized approach is presented in [8], consisting in a *time division multiple access* (TDMA) protocol that dynamically adjusts the sensors transmissions order and duration within a TDMA frame based on channel and traffic status. The objective of this protocol is the minimization of both, the effect of long channel fades and the energy consumption. However, the performance of this proposal depends on the TDMA frame length and, although the significance of this parameter is analyzed, its duration is fixed. On the contrary, the proposed resource allocation scheme considers the effect of the TDMA frame length on the energy efficiency and adapts its duration to the network changing conditions. The proposal of Timmons et al. in [9] presents a scheme with an adaptable length of the TDMA slots assigned to sensors in a configurable superframe. Sensors can sleep for long periods thanks to the grouping of their transmissions and easy synchronization, allowing greater energy savings than the ones achievable with the IEEE 802.15.6 MAC layer. However, this MAC protocol can not be supported by any of the current standards and, furthermore, no analytical characterization of its behavior is derived. Both drawbacks are overcome by the work developed by L. Ruan et al. in [5], where the authors present an optimal time framework for periodic scheduled traffic compliant to the SmartBAN MAC definition. Their main aim is to minimize delay whilst improving energy efficiency. In spite of the promising results obtained with this protocol, it is not worth investing energy to shorten delay when this is not a requirement. In contrast, the present proposal, the *eeAlgorithm*, which is based on a preliminary version presented in [11], focuses on reducing the energy consumption of transceivers while satisfying the delay constraints of scheduled and contention traffic. To that end, it derives the duration of the inter-beacon intervals and the transmission periods of sensors, allowing sensors remain in

sleep mode as long as possible. This is achieved by grouping the sensor transmissions within the margins fixed by the delay constraints. This strategy leads to improved energy efficiency and results invariably show high energy savings, specially for sensors that allow long elapsed times between transmission periods, consistently outperforming the values presented in [5].

To overcome the impact of wireless fading channels and to support the diverse QoS requirements of heterogeneous users, adaptive transmission schemes have been widely used over the last decades [12], [13]. Adapting to the channel characteristics can reduce average *packet error rate* (PER) or increase average throughput by taking advantage of favorable channel conditions to transmit at high data rates, that will be reduced as the channel degrades. Several works have proposed some form of link adaptation in the WBAN environment [14], [15], but most of them consider a WBAN using the *Carrier Sense Multiple Access with Collision Avoidance* (CSMA-CA) protocol. Authors in [14] investigate the IEEE 802.15.6 standard, having a PHY layer with various modulation schemes. This paper presents an adaptive transmission strategy as an efficient way to preserve link quality in environments with high interference levels. The hub measures the *Signal-to-Interference and Noise Ratio* (SINR) experienced by all sensors and, according to a predefined set of SINR partitions, it informs sensors about the transmission scheme they ought to use. The main shortcomings of this proposal are twofold; on the one hand, its inability to support sensors with elapsed times between transmissions longer than the channel coherence time; on the other hand, the incapacity of obtaining a SINR partition capable of guaranteeing a given target PER. A similar proposal is presented in [15] for a WBAN based on the use of the IEEE 802.15.4 standard. Channel quality is observed in terms of *Signal-to-Noise Ratio* (SNR), and a query-based scenario is considered, where the nodes have to send one fixed-size packet whenever the coordinator requests it. Link adaptation is introduced with the aim of reducing packet losses. The present proposal differs substantially from these previous works as it investigates the effect of link adaptation over periodic scheduled traffic in a WBAN following the specifications of the ETSI SmartBAN standard. Therefore, and making use of the availability of six different *transmission modes* (TMs) in the SmartBAN PHY layer specification [2], an adaptive TM selection algorithm is proposed that, depending on the current channel conditions and taking into account the QoS requirements in terms of target PER, determines the transmission scheme to be used. In contrast to the previously mentioned works, the present proposal fulfills the PER requirements of all sensors. Furthermore, it distributes the implementation of the algorithm in both, hub and sensors, by adapting the analysis described in [16] for mobile networks, to the WBAN environment. As a result, this scheme partially decentralizes the TM decision making, allowing long duty cycle sensors support. Moreover, the effect of the different SmartBAN PHY layer specification TMs on delay and energy consumption is thoroughly analyzed.

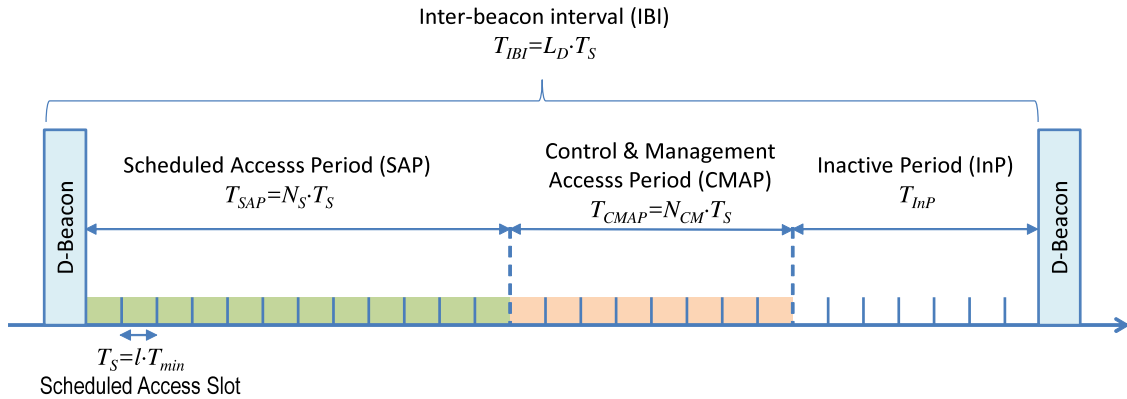


FIGURE 1. SmartBAN data channel (DCH) and inter-beacon interval (IBI) structure.

To the best of our knowledge, there is no previous SmartBAN study that tackles both, the PHY transmission mode selection and the MAC layer configuration adjustment, in a simultaneous and comprehensive analysis. To that end this paper aims at investigating the effects of adapting the MAC parameters for SmartBAN systems using an adaptive transmission scheme at the PHY layer, to improve energy efficiency while maintaining the traffic QoS requirements in terms of PER and delay.

The organization of this paper is as follows. The main characteristics of the SmartBAN MAC protocol are briefly described in Section II. Next, Section III introduces the considered packet transmission model, as well as the SmartBAN standard PHY layer TMs. An accurate analytic approximation of the PER corresponding to all these TMs is also derived. Based on these previous results, Section IV presents a very simple adaptive transmission algorithm to select the most appropriate TM to be used at both, hub and sensors. The system model is introduced in Section V, where the proposed *ee*Algorithm is presented and analytic expressions for traffic delay, energy savings and battery lifespan are provided. Section VI is devoted to the performance analysis of the proposed framework and its comparison with the work presented in [5]. The main conclusions and forthcoming work are described in Section VII.

II. ETSI SmartBAN MAC PROTOCOL

This Section provides a general overview of the SmartBAN MAC layer and interested readers are referred to [3] for a detailed description of the technical specification of the standard. Two different device types can participate in a SmartBAN: up to 16 medical sensor devices (known as *nodes*) and one coordinator device (the *hub*). The network is organized using a star topology with at least one node connected directly to the hub. In this standard, all uplink and downlink data transmissions are performed through a *data channel* (DCH). As shown in Fig. 1, the DCH is organized in frames separated with *data channel beacons* (D-Beacon), broadcasted by the hub. These frames are denoted as *inter-beacon intervals* (IBI) and have a duration of T_{IBI} seconds. The IBI is composed of L_D time slots of duration T_S seconds. Each slot contains l slot

TABLE 1. Notation used in the paper.

Symbol	Meaning
T_{IBI}	IBI duration
L_D	Number of time slots in one IBI
T_S	Time slot duration
N_S	Number of time slots in the SAP
N_{CM}	Number of time slots in the CMAP
T_{SAP}	Time duration of the SAP
T_{CMAP}	Time duration of the CMAP
T_{InP}	Time duration of the InP
L_F	Number of bits in the MAC frame body
γ_ν	Instantaneous received SNR
γ_n^m	TM selection thresholds mode n is selected when $\gamma_\nu \in [\gamma_n^m, \gamma_{n+1}^m)$
Γ^m	Set of non-overlapping intervals of the SNR range $\Gamma^m = \{[\gamma_0^m, \gamma_1^m), [\gamma_1^m, \gamma_2^m), \dots, [\gamma_{M-1}^m, \gamma_M^m)\}$
T_G	Sensors data generation periods set
T_{g_i}	Elapsed time between successive sensing intervals of node i
V_D	Sensors data volumes set
V_{d_i}	Number of data bits sensor i generates during a sensing interval
D_M	Sensors data delay requisites set
D_{m_i}	Maximum allowed delay for sensor i traffic
T_T	Sensors transmission periods set
T_{t_i}	Elapsed time between successive scheduled transmissions of sensor i
W_M	Sensors allowed waiting times set
W_{m_i}	Maximum amount of time sensor i can wait to transmit its packets
l_{s_i}	Number of allocated slots to sensor i
T_{SF}	WBAN superframe duration
D_E	Maximum delay that emergency traffic can afford
D_i	Average delay experienced by sensor i
η_{s_i}	Energy savings for sensor i
η_{hub}	Energy savings for the hub
$T_{Battery_i}$	Sensor i battery lifetime

units of duration $T_{min} = 625\mu s$, that is, $T_S = l * T_{min}$, being $l = 2^b$ ($b = 0, 1, 2, 3, 4, 5$). The L_D IBI time slots are grouped into three periods: $N_S \geq 0$ time slots conform the *scheduled access period* (SAP, corresponding to TDMA scheduled data transmissions), $N_{CM} > 0$ time slots are reserved for the *control and management access period* (CMAP, corresponding to unscheduled data transmissions, and management and control signaling), and the rest of the IBI time slots, if there are any, form the *inactive period* (InP, no transmissions). T_{IBI} , N_S , N_{CM} and l are all tunable parameters. Table 1 summarizes the notation used throughout this paper.

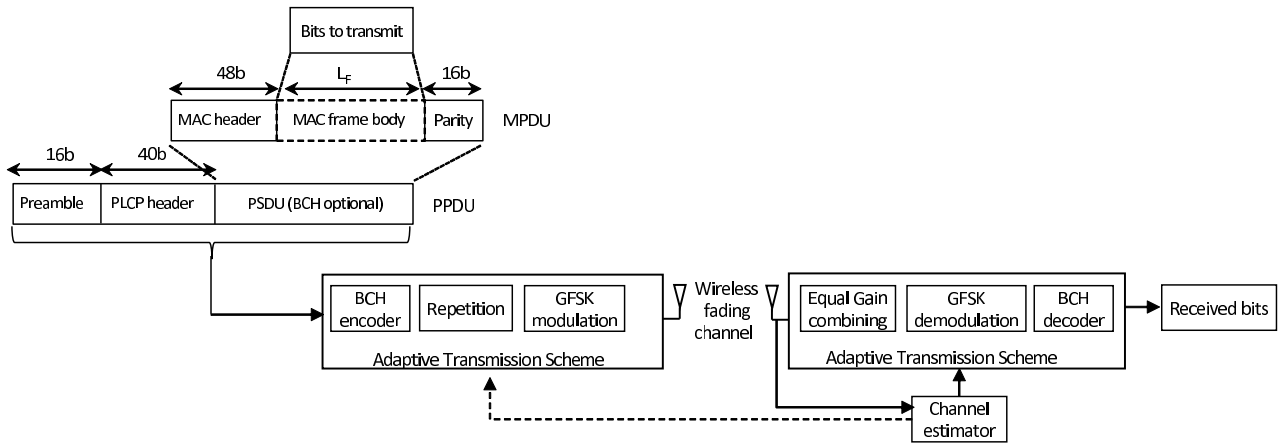


FIGURE 2. SmartBAN communication system block diagram.

The SmartBAN technical specification differentiates among three types of channel access: *Scheduled Channel Access* (SChA), *Slotted Aloha Channel Access* (SACHA) and *Multi-Use Channel Access* (MUCHA), used in the SAP period, in the CMAP period, and in both, respectively. The proposed framework corresponds to the SChA method used in the SAP period, as it is the most suitable mode for the predominant periodic traffic. In SChA a sensor can reserve time slots in the SAP by using a C-Req message to request a connection to the hub. With a C-Ass message, the hub informs the sensor about the scheduled access grant, identifying scheduled SAP slots. Both the C-req and C-Ass messages are transmitted in the CMAP period. The C-Ass hub message includes the sequence number of the initial IBI when the sensor needs to wake up, and the number of IBIs between successive wake up instants. This procedure supports sensors having off periods longer than T_{IBI} . Moreover, the standard allows changes in this initial assignment through a slot reassignment list present in the D-Beacon. Changes are continuously broadcasted in consecutive D-beacons until the intended nodes acknowledge reception. The proposed resource allocation algorithm benefits from these SmartBAN features to reduce hub and sensors power consumption.

III. BER AND PER DERIVATION

A. SmartBAN PACKET TRANSMISSION MODEL

Fig. 2 represents the smartBAN packet communication system under consideration, highlighting the main blocks involved in the communication process. Data generated by sensors are transmitted using the MAC frame, known as *MAC Protocol Data Unit* (MPDU). MAC frames consist of a sequence of a MAC header of 48 bits, a MAC frame body of length L_f bits (only present if it has a nonzero length), and a frame parity of 16 bits [3].

The *Physical Layer Protocol Data Unit* (PPDU) starts with a 16-bit preamble for frequency and timing synchronization as well as for automatic gain control, followed by a 40-bit *Physical Layer Convergence Protocol* (PLCP) header and the *Physical Layer Service Data Unit* (PSDU), corresponding to

the MPDU. A systematic BCH(127,113, $t = 2$) code can be used for error correction control of MPDU, being t the maximum number of correctable bits [2].

According to the SmartBAN PHY layer specification, repetition coding at hub and nodes may be implemented, if required [2]. 2-repetitions and 4-repetitions of the PPDU are supported, treating the original PPDU and its repetitions as one single PPDU. *Gaussian Frequency Shift Keying* (GFSK) with modulation index $h = 0.5$ and a bandwidth-bit period product $BT = 0.5$, is used, supporting a symbol rate of 1 MSymb/s.

Let us assume that in the k th signaling period a symbol s_k is transmitted, with $E_T = |s_k|^2$ denoting the energy per transmitted symbol. A generic wireless fading channel is considered, which is characterized by h_k , representing the complex-valued baseband equivalent fading during the k th signaling period. The received signal can be expressed as $r_k = s_k h_k + n_k$, where n_k is a complex additive white Gaussian noise (AWGN) sample with zero mean and variance $N_0/2$ per dimension. The instantaneous received SNR at time instant $t = \nu T_{IBI}$ with $\nu \in N^+$ is defined as $\gamma_\nu = E_T |h_\nu|^2 / N_0 = E_S / N_0$, where $E_S = E_T |h_\nu|^2$ denotes the energy of the received signal.

The considered adaptive transmission scheme determines the TM to be used, which corresponds to the combination of a number of repetitions of the PPDU, and the use or not of BCH coding for the MPDU. Perfect channel state information is considered to be available at the receiver side in terms of the received SNR, γ_ν . Then, a TM selection process is performed at the receiver adaptive transmission scheme controller and fed back to the transmitter, as will be detailed in the following Section.

At the receiver end, PPDU's are added together by using the *Equal Gain Combining* (EGC) scheme, supposing perfect channel phase estimation. An optimum GFSK demodulator has been assumed, where a correlator is followed by a *maximum likelihood sequence detector* (MLSD). Subsequent to removing preamble and header, the BCH decoder decodes the received bits.

TABLE 2. ETSI SmartBAN Transmission Modes (fitting parameters with $L_f = 200$ bytes).

	TM6	TM5	TM4	TM3	TM2	TM1	TM0
Modulation	GFSK	GFSK	GFSK	GFSK	GFSK	GFSK	No transmission
PPDU repetitions	1	1	2	2	4	4	-
MPDU BCH-coding	No	Yes	No	Yes	No	Yes	-
a_n	85.8840	703.4663	55.6195	904.5274	97.2746	1818.7753	-
g_n	0.8462	1.7757	1.6574	3.7711	3.7251	8.1808	-
γ_{p_n} (dB)	7.2117	5.6725	3.8463	2.5651	0.8948	-0.3739	-
Information rate (Mbps)	1.00	0.89	0.50	0.44	0.25	0.22	-

B. TRANSMISSION MODES POOL AND CHARACTERIZATION OF THE PACKET ERROR RATE

As already mentioned, the ETSI SmartBAN Standard allows the use or not of BCH coding for the MPDU and the possibility of PPDU repetition. These capabilities give birth to the six PHY transmission modes summarized in Table 2. The PHY Scheme field in the PLCP header informs about the used TM. In order to characterize these TMs, Packet Error Rate (PER) analytical expressions for all available TMs will be derived.

The PHY layer instantaneous PER at the output of the BCH decoder will depend on the selected TM and on the instantaneous received SNR. The PER of these TMs can be approximated as [16]–[19]:

$$PER_n(\gamma_v) \approx \begin{cases} 1, & 0 \leq \gamma_v < \gamma_{p_n} \\ a_n e^{-g_n \gamma_v}, & \gamma_v \geq \gamma_{p_n} \end{cases} \quad (1)$$

where γ_v denotes the instantaneous received SNR at time instant $t = \nu T_{IBI}$ with $\nu \in N^+$, and a_n, g_n and γ_{p_n} being the fitting parameters for TM n .

In order to determine PER_n , the ratio between the total number of packet errors and the total number of transmitted packets has been calculated considering different values of L_f , for all available TMs. Fig. 3 plots the instantaneous PER curves corresponding to the six TMs of the ETSI SmartBAN standard, for a MAC frame body length $L_f = 200$ bytes. Graphs obtained through Monte-Carlo simulation are plotted with markers, while the curves obtained by least-squares fitting expression (1) to the simulation results are plotted with

solid lines. The derived fitting parameters a_n, g_n and γ_{p_n} , are listed in Table 2. It is clear from Fig. 3 that the analytical PER expression in (1) accurately approximates the exact instantaneous PER obtained by simulation for all the six available TMs, especially for PER values below 10^{-1} . It is worth noting that higher error rates could never be assumed in real WBANs and, therefore, are of no interest in practical scenarios.

IV. PROPOSED TRANSMISSION MODE SELECTION ALGORITHM

The SmartBAN standard does not describe how the selection between its available PHY modes has to be performed. To tackle this challenge, a very simple adaptive transmission algorithm is proposed, which can be used by both, hub and sensors, for that purpose. The adaptive transmission scheme has a set $\mathcal{M} = \{0, \dots, M - 1\}$ of $M = 7$ TMs, detailed in Table 2. TM 0 represents the case of no transmission, and the rest correspond to a particular combination of number of repetitions of the PPDU, and use or not of BCH coding for the MPDU.

Similarly as in [16], when implementing the adaptive transmission scheme, the entire SNR range is partitioned into a set of non-overlapping intervals defined by the partition

$$\Gamma^m = \{[\gamma_0^m, \gamma_1^m), [\gamma_1^m, \gamma_2^m), \dots, [\gamma_{M-1}^m, \gamma_M^m)\}, \quad (2)$$

with $\gamma_0^m = 0$ and $\gamma_M^m = \infty$. Then, as illustrated in Fig. 4, mode n is selected when $\gamma_v \in [\gamma_n^m, \gamma_{n+1}^m)$.

The adaptive transmission scheme will be designed with the objective of maximizing the data rate while keeping the instantaneous PER below a prescribed value P_0 . According to [16], the partition boundaries Γ^m will be obtained as the minimum received SNR required to achieve P_0 , as illustrated in Fig. 4. Inverting the $PER_n(\gamma_v)$ expression in (1) it can be shown that

$$\begin{cases} \gamma_0^m = 0 \\ \gamma_n^m = \frac{1}{g_n} \ln\left(\frac{a_n}{P_0}\right), & n = 1, \dots, M - 1 \\ \gamma_M^m = \infty \end{cases} \quad (3)$$

To graphically illustrate the proposed link adaptation algorithm with an example, a target PER value $P_0 = 10^{-2}$ is considered in Fig. 4. The graph plots the intersections of the PER curves corresponding to all six available TMs with the horizontal line corresponding to the target PER. These intersecting points constitute the TM switching thresholds, which correspond to the linear values $\Gamma^m = \{0, 1.4804, 2.4650, 3.0263, 5.2031, 6.2853, 10.7045, \infty\}$. Additionally, an horizontal line has been added at the bottom of Fig. 4 showing the

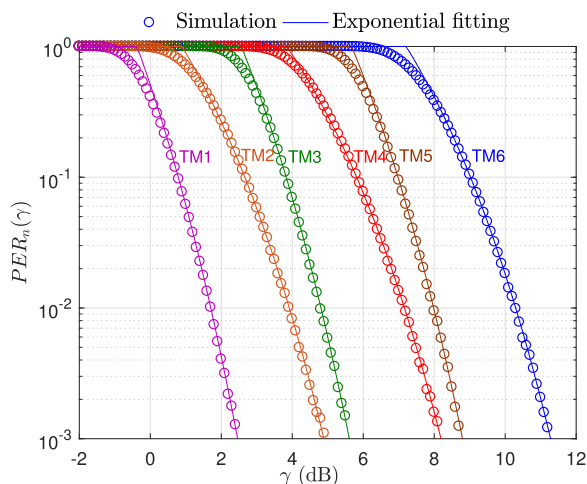


FIGURE 3. Instantaneous PER vs. received SNR, with $L_f = 200$ bytes - ETSI SmartBAN.

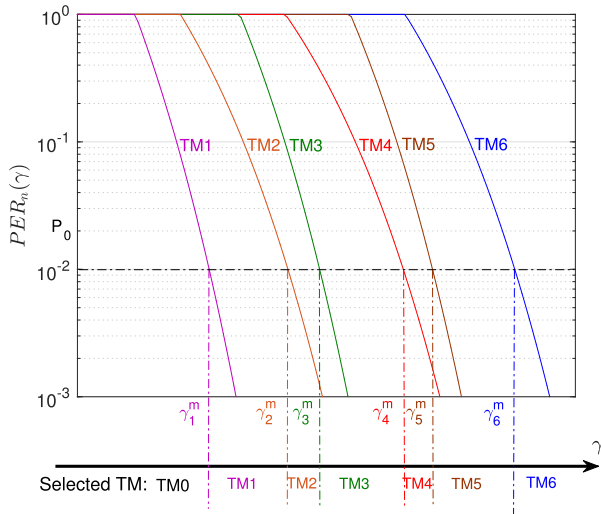


FIGURE 4. Transmission mode selection thresholds.

TM that ought to be selected in each of the obtained partition intervals of the received SNR range.

In order to implement the proposed TM selection algorithm, during the connection process, the hub, using expression (3), computes the partition boundaries corresponding to the target P_0 required by the sensor. The long coherence times and the high correlation between uplink and downlink channels in WBANs [20] make it possible to exploit channel reciprocity. The D-Beacon transmissions performed by the hub allow sensors to estimate the channel quality in terms of received SNR, γ_v . In order to guarantee their target PER requirements, sensors have to select the TM to be used in their uplink transmissions (from sensors to hub) according to the SNR that will be received at the hub. To that end, and taking into account that sensors know the power transmitted by the hub to perform the D-beacon broadcasting, each sensor derives the respective received SNR at the hub by scaling the measured received SNR at the sensor by a factor corresponding to the ratio among hub and sensor transmitted powers. Following this simple procedure, each sensor derives the corresponding received SNR at the hub, which is compared to the partition boundaries, Γ^m , to determine the TM to be used for its uplink transmission. The sensor indicates the selected TM to the hub through the PHY-Scheme field in the PLCP header of the PPDU [2].

The above mentioned procedure takes for granted that perfect channel state information is available at the receiver side in terms of the received SNR, γ_v . However, since in a real scenario the received SNR is just an estimate of the actual SNR, sensors should back off on the estimated SNR in order to reduce the probability of outage [21]. A straightforward strategy to achieve this goal consists of simply increasing the switching thresholds, Γ^m , by a constant, resulting in improved PER performance [22]. A reduction in the correlation between estimated and actual SNR values causes an increase in the PER since the actual SNR may fall into a lower SNR interval than the estimated SNR. This means

that the actually selected TM is not as robust as required to fulfill the target PER P_0 . Although this cannot be completely avoided with any AMC strategy, it is desirable to control the probability of this event, which can be expressed as:

$$P(\gamma_{v,actual} < \gamma_n^m | \gamma_v \in [\gamma_n^m, \gamma_{n+1}^m]) < \epsilon \quad (4)$$

where ϵ is a constant left at the designers' choice. Thus, by increasing the switching thresholds, Γ^m , to obtain a certain desired ϵ , the probability of an AMC mismatch can be reduced in a controlled manner.

Therefore, the optimum amount of back off that maximizes the throughput while fulfilling the target PER requirements should be computed as a function of the estimation error. This procedure constitutes a research work itself, falling out of the scope of the present paper and, therefore, it is left for a future research.

V. PROPOSED RESOURCE ALLOCATION SCHEME

A. SYSTEM MODEL

The considered SmartBAN networks consists of N nodes that periodically measure body parameters and transmit the information to the hub. This smartBAN is characterized by the following sets:

- data generation periods, $T_G = \{Tg_1, Tg_2, \dots, Tg_N\}$, where Tg_i corresponds to the elapsed time between successive sensing intervals of node i ;
- data volumes, $V_D = \{Vd_1, Vd_2, \dots, Vd_N\}$, where Vd_i specifies how many data bits sensor i generates during a sensing interval;
- data delay requisites, $D_M = \{Dm_1, Dm_2, \dots, Dm_N\}$, where Dm_i denotes the maximum allowed delay for sensor i traffic.

The standard defines a slot structure for the SAP period consisting of a data transmission period, an ACK transmission period and two *inter-frame spaces* (IFS) [3]. As a result, the required slot time duration for sensor i is

$$Ts_i = T_{DATAi} + T_{ACK} + 2T_{IFS}, \quad (5)$$

where $T_{ACK} = 120 \mu s$, $T_{IFS} = 150 \mu s$ are both fixed by the SmartBAN standard specifications, and T_{DATAi} can be obtained as follows:

$$T_{DATAi} = T_{PPDUi} \cdot N_{REPi} = \frac{L_{PPDUi}}{R_{sym}} \cdot N_{REPi}, \quad (6)$$

where $N_{REPi} = \{1, 2, 4\}$ indicates the number of repetitions of the PPDU, that will be determined according to the proposed TM selection algorithm presented in IV, and $R_{sym} = 1\text{Msymb/s}$ is the symbol rate.

Besides, as illustrated in Fig. 2, $L_{PPDUi} = L_{preamble} + L_{PLCPHdr} + L_{PSDUi}$, with

$$L_{PSDUi} = \begin{cases} L_{MPDUi}, & \text{uncoded} \\ \left\lceil \frac{L_{MPDUi}}{k} \right\rceil (n-k) + L_{MPDUi}, & \text{BCH}(n,k) \end{cases} \quad (7)$$

where $\lceil x \rceil$ denotes the nearest integer greater than or equal to x , and $L_{MPDUi} = L_{MACHdr} + L_{Fi} + L_{parity}$, with the MAC

frame body length of sensor i corresponding to $L_{Fi} = Vd_i$. The use or not of BCH coding will depend on the selected TM, as proposed in IV.

Using eqs. (5) to (7), the slot length necessary for each sensor, Ts_i , with $i = \{1, 2, \dots, N\}$, can be obtained. Finally, to determine the actual slot duration, the possible existence of MAC frame body fragmentation needs to be considered:

$$Ts = \begin{cases} \max\{Ts_i, i = \{1, \dots, N\}\} & \text{s.t. } Ts = IT_{min}, \text{ no frag.} \\ \min\{Ts_i, i = \{1, \dots, N\}\} & \text{s.t. } Ts = IT_{min}, \text{ frag.} \end{cases} \quad (8)$$

Therefore, the number of allotted slots to sensor i , ls_i , can be obtained as:

$$ls_i = \left\lceil \frac{Ts_i}{Ts} \right\rceil. \quad (9)$$

B. PROPOSED eeAlgorithm

The IBI length T_{IBI} is a critical MAC parameter that heavily affects the energy consumption of hub and sensors. In fact, it was shown in [5] that T_{IBI} is inversely proportional to the energy consumption. As a result, the main objective of the *eeAlgorithm* is to extend as much as possible the IBI length while still ensuring the delay requirements of the different traffic types. This is accomplished by grouping a certain number of data generation periods of each sensor to form its *transmission period*, $Tt_i = G_i * Tg_i$, where $G_i \in N^+$ denotes the number of grouped generation periods for sensor i . Therefore, Tt_i corresponds to the elapsed time between successive scheduled transmissions of sensor i . The set of transmission periods is defined as $T_T = \{Tt_1, Tt_2, \dots, Tt_N\}$.

The maximum amount of time a sensor can wait to transmit its packets is denoted as Wm_i and the set of waiting times characterizing the smart WBAN is expressed as $W_M = \{Wm_1, Wm_2, \dots, Wm_N\}$. Wm_i can be obtained as $Wm_i = Dm_i - T_{BAN} - T_{NET}$, where T_{BAN} is defined as the average required time for a successful transmission from sensor to hub (severely dependent on the radio channel quality), and T_{NET} is the transmission time from hub to the destination server. In the present work it has been considered that $W_M = D_M$, and T_{BAN} and T_{NET} will be left for future research.

The *eeAlgorithm* is depicted in Fig. 5. Let us define the set $M = \{m_1, m_2 \dots m_l\}$, with $m_t > m_{t+1}$, composed by the multiples of all possible combinations of products of the prime factors of T_{IBI}^{min} , f_1, f_2, \dots, f_k , in the range $[T_{IBI}^{min}, T_{IBI}^{max}]$, where $T_{IBI}^{min} = GCD(T_G)$ (with *GCD* being the *greatest common divisor*) and $T_{IBI}^{max} = min(W_M)$. The procedure starts with an IBI candidate equal to the highest multiple, m_1 , within the T_{IBI} range. Next, the algorithm checks if this T_{IBI} value fulfills all the traffic requirements. In case they are met, this T_{IBI} candidate constitutes the IBI duration obtained with the *eeAlgorithm*. Otherwise, the next possible multiple is considered and the algorithm checks if this new T_{IBI} candidate fulfills all the traffic requirements. This process is performed until a valid T_{IBI} is obtained. If the minimum IBI is reached without meeting all the conditions,

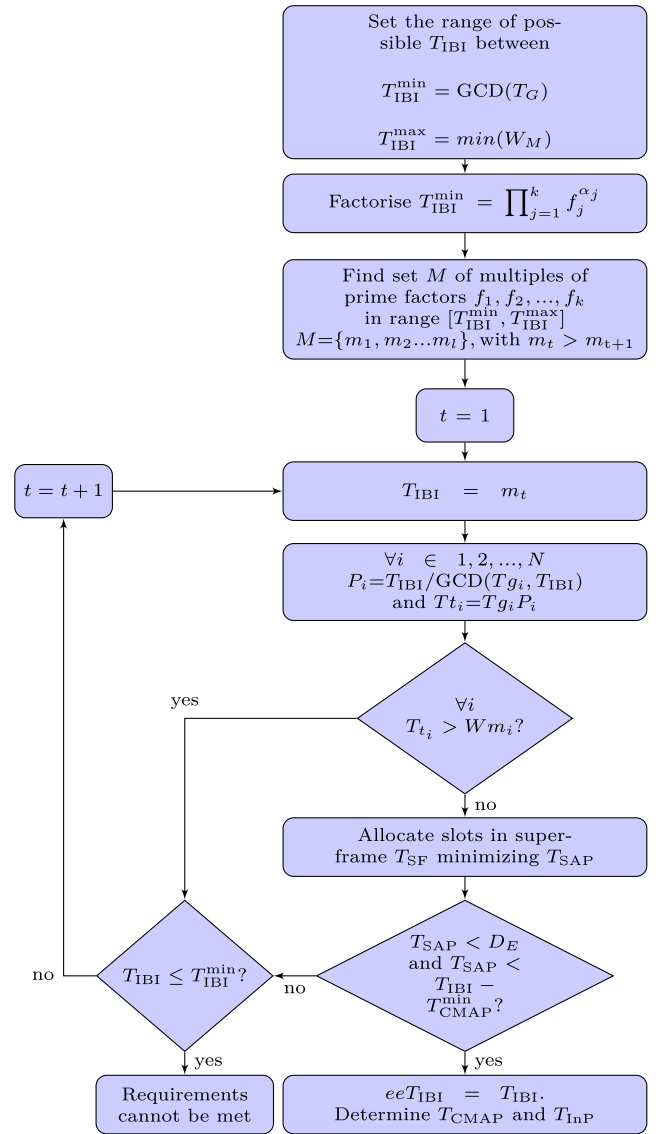


FIGURE 5. eeAlgorithm flowchart.

then the traffic requirements cannot be met with the actual configuration (number of nodes, expected alert messages delay, etc.). As the minimum possible IBI corresponds to $GCD(T_G)$, in case the *eeAlgorithm* reaches the last iteration, it reverts to the *optimal-IBI* solution proposed in [5], and no grouping is performed ($T_T = T_G$). Therefore, if in that last iteration the requirements are still not met, it means that the resultant T_{SAP} period is too long (too many periodical packets transmissions), and the emergency delay, D_E , or the minimum required CMAP interval, T_{CMAP}^{min} , can not be achieved. In this case, the hub will have to limit the amount of traffic from each sensor or relax the delay requirements.

As represented in Fig. 5, at each iteration the proposed algorithm:

- 1) Determines, for all sensors, the number of grouped generation periods as $G_i = T_{IBI}/GCD(Tg_i, T_{IBI})$, and obtains the transmission period of each sensor as $Tt_i = Tg_i G_i$.

- 2) Verifies that the transmission periods Tt_i of all sensors are lower or equal than their maximum allowed waiting times Wm_i .
- 3) The IBI duration, T_{IBI} , and the set of transmission periods, T_T , define a WBAN superframe with duration $T_{SF} = n * T_{IBI} = LCM(T_T)$, where $n \in N^+$ and LCM being the *least common multiplier* of set T_T . The criterion followed to determine the initial IBI when each sensor has to start transmission within the superframe, $T_{IBI,i}^{ini}$, is the minimization of the T_{SAP} period, that is, the maximum number of SAP slots in an IBI within the superframe. Then, l_{s_i} slots are allocated to sensor i each $T_{IBI,i}^{ini} + p * Tt_i$, $p \in N$, for all sensors in the SmartBAN.
- 4) Next, it is mandatory to consider the maximum delay that emergency traffic can afford, D_E . This maximum delay occurs when the message is created at the start of the InP, because it will have to wait till next CMAP to be sent, $D_E = T_{SAP} + T_{InP}$. As the T_{InP} can be arbitrarily set to zero, then it is mandatory that $T_{SAP} < D_E$ to fulfill the emergency traffic delay requirement. Moreover, it has to verify that the IBI includes a minimum CMAP interval $T_{IBI} - T_{SAP} > T_{CMAP}^{min}$.
- 5) Finally, the CMAP and InP durations are determined as follows:
 - if $T_{IBI} > D_E$ then $T_{CMAP} = T_{IBI} - D_E$;
 - else if $T_{IBI} > 2 \cdot T_{SAP}$ then $T_{CMAP} = T_{SAP}$.
 And, obviously, $T_{InP} = T_{IBI} - T_{SAP} - T_{CMAP}$.

As an example, let us consider a system with three sensors with generation times $T_G = \{1500, 250, 300\}$ ms and data delay requisites $D_M = \{3, 1, 1.5\}$ s. Supposing a slot length $T_S = 1.25$ ms and that all sensors require $l_{s_i} = 8$ slots to transmit the data of a sensing interval, these transmissions will last 10 ms each one. The algorithm starts with a $T_{IBI} = 1$ s, the largest T_{IBI} candidate, corresponding to the most stringent delay requirement. For this T_{IBI} , the grouping indexes for the three sensors are $G_1 = 2$, $G_2 = 4$ and $G_3 = 10$, and the obtained transmission times are $T_T = \{3000, 1000, 3000\}$ ms, respectively. As the resulting transmission time for sensor 3 ($T_{T_3} = 3$ s) exceeds the delay requirement for that sensor ($D_3 = 1.5$ s), the next multiple in set M is checked. After several iterations, when a $T_{IBI} = 750$ ms is tested, the obtained grouping indexes are $G_1 = 1$, $G_2 = 3$ and $G_3 = 5$, and the resulting transmission times are $T_T = \{1500, 750, 1500\}$ ms, respectively, all of them fulfilling their delay requirements. Therefore, sensor 1 will transmit its sensing data every time it is generated, that is, every 1500 ms; sensor 2 will group its sensing data corresponding to 3 consecutive generating periods, which will be transmitted every 750 ms; finally, sensor 3 will group 5 consecutive sensing measurements to be transmitted every 1500 ms. The superframe duration is $T_{SF} = LCM(T_T) = 1500ms$, corresponding to two T_{IBI} s. The sensors slots are organized in the superframe with the aim of minimizing the T_{SAP} period, as shown in Fig. 6, yielding a $T_{SAP} = 80ms$. Considering a maximum affordable delay for emergency traffic $D_E = 100$ ms, the requirement $T_{SAP} < D_E$ is fulfilled.

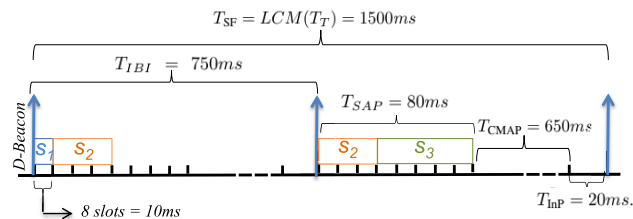


FIGURE 6. Example configuration of MAC parameters.

Moreover, as $T_{IBI} > D_E$, the control period duration is $T_{CMAP} = 650ms$, and the inactive period $T_{InP} = 20ms$.

This is a $O(n)$ algorithm, where n corresponds to the size of the set of possible multiples, M . Taking into account that the medical sensors sampling times and maximum delays in all realistic scenarios [23] result, in the worst of cases, in a set M including only a few hundred elements, a small and bounded running time will result in all practical cases. It should be pointed out that this simple algorithm is executed by the hub, never by a sensor node, every time a new connection or disconnection request is transmitted by the sensors. Following the slot-reassignment MAC function described in the SmartBAN standard [3, Section 7.5], the hub announces the new slot allocation and informs the corresponding sensor nodes.

C. PERFORMANCE PARAMETERS

Analytical expressions for delay, energy savings and battery lifespan were derived in the preliminary work presented in [11]. An overall description of the obtained formulas will be provided, and readers are referred to the aforementioned paper and references therein for further details.

Delay experienced by the j_{th} data generation period of sensor i , $D_{i,j}$, corresponds to the elapsed time between the data generation and the start of transmission (plus transmission time). It can be calculated as:

$$D_{i,j} = Tt_i \cdot u(t_{i,j} - Ts \cdot k_i) + Ts \cdot (k_i + jls_i) - t_{i,j}, \quad (10)$$

where

$$t_{i,j} = m_i Ts + (j - 1)Tg_i, \quad (11)$$

with m_i being sensor's i first data generated within T_{IBI} , k_i its first allocated slot within T_{IBI} , and $u(\cdot)$ the unit step function.

The number of times sensor i generates data within its transmission period can be obtained as the ratio $Mg_i = Tt_i/Tg_i$. Therefore, the average delay experienced by sensor i , D_i , can be derived by averaging the corresponding $D_{i,j}$ values as follows:

$$D_i = \frac{1}{Mg_i} \sum_{j=1}^{Mg_i} D_{i,j}. \quad (12)$$

Energy savings of sensor i can be obtained as (13), as shown at the bottom of the next page, where the pairs $\{P_{ACTV_s}, T_{ACTV_i}\}$, $\{P_{SLP_s}, T_{SLP_i}\}$ and $\{P_{SW_s}, T_{SW_i}\}$, correspond to the consumed powers and time intervals when sensor i is in active mode, in sleeping mode, and when it

switches between both, respectively. These time intervals are derived as follows:

$$T_{ACTV_i} = Mt_i \cdot T_{D_{bcn}} + Mg_i \cdot ls_i \cdot Ts, \quad (14)$$

$$T_{SW_i} = 2(Mt_i + 1) \cdot T_{SW}, \quad (15)$$

$$T_{SLP_i} = Tt_i - T_{ACTV_i} - T_{SW_i}, \quad (16)$$

with $Mt_i = Tt_i/T_{IBI}$, $T_{D_{bcn}}$ being the D-Beacon frame duration and T_{SW} the time for a node to switch.

Similarly, the hub energy savings can be calculated as:

$$\eta_{hub} = \left(1 - \frac{T_{ACTV_{hub}} \cdot P_{ACTV_{hub}} + T_{DZ_{hub}} \cdot P_{DZ_{hub}}}{T_{SF} \cdot P_{ACTV_{hub}}} \right), \quad (17)$$

where the pairs $\{P_{ACTV_{hub}}, T_{ACTV_{hub}}\}$ and $\{T_{DZ_{hub}}, P_{DZ_{hub}}\}$, correspond to the time intervals and corresponding power consumption in which hub is in active mode and in doze mode, respectively. These time intervals are:

$$T_{ACTV_{hub}} = \sum_{i=1}^N \frac{T_{SF}}{Tt_i} \cdot Mg_i \cdot ls_i \cdot Ts + \frac{T_{SF}}{T_{IBI}} \cdot T_{D_{bcn}}, \quad (18)$$

$$T_{DZ_{hub}} = T_{SF} - T_{ACTV_{hub}}. \quad (19)$$

Finally, considering sensor i has a battery of capacity $Q_{Battery_i}$ mAh, its lifetime can be derived as:

$$T_{Battery_i} = \frac{Q_{Battery_i}}{Q_{TOTAL_i}} \cdot Tt_i, \quad (20)$$

with

$$\begin{aligned} Q_{TOTAL_i} &= Mt_i \cdot T_{D_{bcn}} \cdot I_{Rx} \\ &+ Mg_i \cdot ls_i \cdot (T_{Data} \cdot I_{Tx} + T_{ACK} \cdot I_{Rx} + 2T_{IFS} \cdot I_{Wait}) \\ &+ (1 + Mt_i) \cdot T_{Wup} \cdot I_{Wup} + T_{Slp_i} \cdot I_{Slp}, \end{aligned} \quad (21)$$

where sensor drawn current for reception, transmission, wait, wake up and sleep are I_{Rx} , I_{Tx} , I_{Wait} , I_{Wup} and I_{Slp} , respectively. The required time intervals are:

$$T_{Data} = Ts - T_{ACK} - 2T_{IFS}, \quad (22)$$

$$T_{Slp_i} = Tt_i - (Mt_i \cdot T_{D_{bcn}} + Mg_i \cdot ls_i \cdot Ts + (1 + Mt_i) \cdot T_{Wup}), \quad (23)$$

and T_{Wup} corresponds to the wake up time.

VI. PERFORMANCE EVALUATION

This section is devoted to the analysis of the proposed link adaptation scheme and *eeAlgorithm* introduced in Sections IV and V, respectively. As already mentioned in Section I, just the proposal of L. Ruan et al. in [5] analyzes periodic traffic performance in the SmartBAN standard and, therefore, it will constitute the reference framework for comparison with the results obtained with the present research

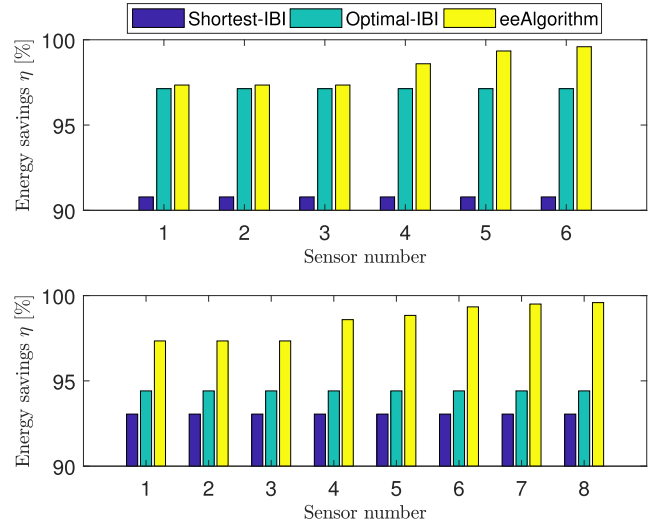


FIGURE 7. Energy savings for 6 and 8 sensors SmartBANs [11].

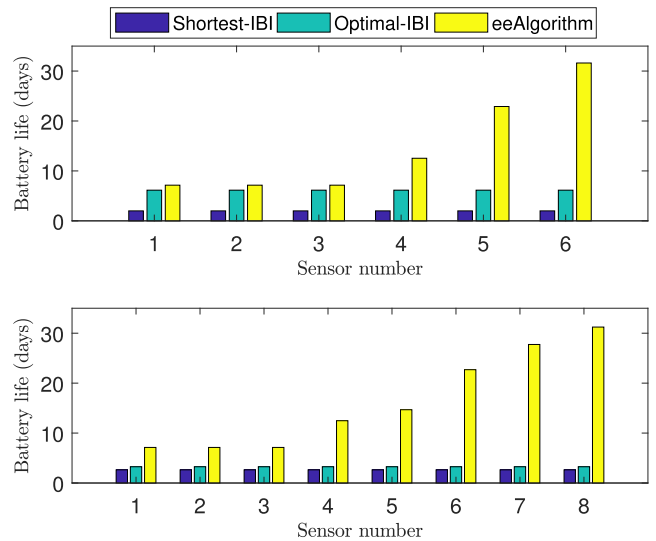


FIGURE 8. Battery lifetime for 6 and 8 sensors SmartBANs [11].

work. Authors in [5] presented the *shortest-IBI*, obtained by setting $T_{CMAP} = T_{SAP}$ with $T_{INP} = 0$, and the *optimal-IBI*, which was achieved by setting $T_{IBI} = GCD\{Tg_i, i = 1, 2, \dots, N\}$ and extending T_{INP} accordingly. Simulations have been conducted using Matlab® [24]. Unless otherwise specified, numerical results will be obtained for a default MAC frame body length $L_f = 200$ bytes and fragmentation is allowed.

A. ENERGY SAVINGS AND BATTERY LIFETIME ANALYSIS AND COMPARISON

To ease an accurate comparison with the proposal presented in [5], the same SmartBANs composed of 6 and 8 on-body sensors, with characteristics detailed in ([5], Tables II-III), will be analyzed. $D_E = 200$ ms and $Dm_i = 3$ s for all

$$\eta_{s_i} = \left(1 - \frac{T_{ACTV_i} \cdot P_{ACTV_s} + T_{SLP_i} \cdot P_{SLP_s} + T_{SW_i}(2 + 2Mt_i) \cdot P_{SW_s}}{Tt_i \cdot P_{ACTV_s}} \right), \quad (13)$$

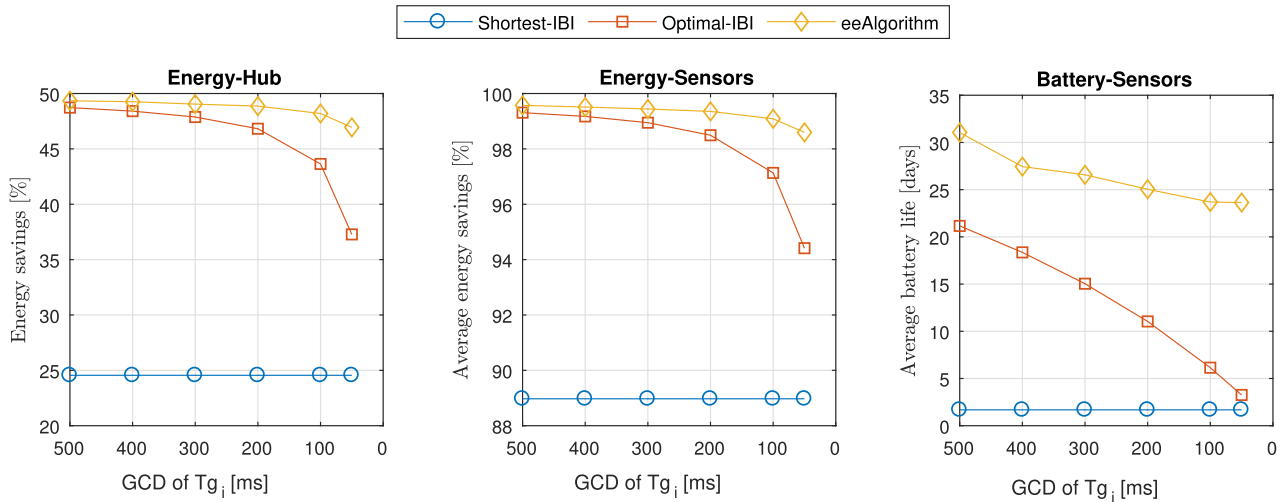


FIGURE 9. Energy savings and battery lifetime vs. GCD of the Tg_i values.

sensors, as specified in [23]. Q_{TOTALi} , T_{Wup} , I_{Rx} , I_{Tx} , I_{Wait} , I_{Wup} and I_{SIP} values are detailed in [4]. In order to compare results corresponding to *shortest-IBI* and *optimal-IBI* with the proposed *eeAlgorithm*, only TM6 will be considered to be used throughout this Subsection.

Results for both scenarios, with 6 and 8 sensor nodes, are plotted in Figs. 7 and 8, showing the energy savings and battery lifetime, respectively, for all sensors, arranged in ascending order of Tg_i . The proposed *eeAlgorithm* outperforms the *optimal-IBI* and *shortest-IBI* proposals. The resulting T_{IBI} values with the three schemes are 2000 ms, 100 ms and 30 ms, respectively, when the SmartBAN with 6 sensors is considered, and 1500 ms, 50 ms and 40 ms for the 8 sensors SmartBAN. From Fig. 7 it can be inferred that the longer the IBI duration, the lower the energy consumed by sensors, as previously mentioned in Subsection V-B. In contrast to the proposal in [5], in which it can be observed the same behavior for all sensors in a given scenario, when the *eeAlgorithm* is considered, longer Tg_i values lead to higher energy savings. The explanation of this behavior is that a sensor with higher Tg_i can stay in sleep mode during longer time periods, increasing the energy efficiency. These results are consistent with the graphs depicted in Fig. 8, showing a significant increase of battery lifespan with the proposed *eeAlgorithm* when compared with the *optimal-IBI* scheme, specially for sensors with higher Tg_i values (a 515% increase for sensor 6 in the first scenario and 960% for sensor 8 in the second scenario is obtained).

The dependence of the energy efficiency on the GCD of the Tg_i values is analyzed in Fig. 9. Six scenarios, each of them with five sensors, have been considered, corresponding to GCDs 500 ms, 400 ms, 300 ms, 200 ms, 100 ms and 50 ms, respectively, as summarized in table 3. The figure plots the energy savings of the hub and the average energy savings and average battery duration of the five sensors, for each scenario. As previously mentioned, in the *shortest-IBI* case, performance does not depend on the GCD

TABLE 3. Scenarios corresponding to Fig. 9.

Scenario	Tg_1	Tg_2	Tg_3	Tg_4	Tg_5	GCD [ms]
1	500	1000	1000	1500	2000	500
2	400	800	1200	1600	2000	400
3	300	600	900	1200	1800	300
4	200	600	1000	1400	2000	200
5	100	500	1000	1400	2000	100
6	50	500	1000	1250	2000	50

value, while when *optimal-IBI* and *eeAlgorithm* are considered, it varies with GCD. Both algorithms yield to better behavior than the *shortest-IBI* scheme and, most importantly, the *eeAlgorithm* outperforms the *optimal-IBI* proposal: the lower the GCD value, the higher this improvement. The reason for this accomplishment is that in the *optimal-IBI* scheme the IBI duration coincides with the GCD value, while with the *eeAlgorithm* T_{IBI} remains higher for all considered scenarios and it results in a reduction of energy consumption. It is important to point out that the hub energy savings depicted in Fig. 9 have been determined considering only the energy consumed in the WBAN. In order to add the required energy to relay the relevant medical data further up in the network, using for example 5G or WiFi technologies, an energy consumption model similar to the one described in [25] should be considered.

B. ANALYSIS OF THE REPETITIONS AND BCH USAGE

With the aim of analyzing the behavior of the *eeAlgorithm* when different number of PPDU repetitions as well as when BCH coding for the MPDU is used, the same SmartBAN with 6 on-body sensors that has been previously considered in Subsection VI-A will be studied. Obtained results will be contrasted with the *optimal-IBI* proposal [5].

Fig. 10 plots the energy savings and battery lifetime for all sensors when TM2, TM4 and TM6 are used (4, 2 and 1 repetitions, respectively, and no BCH coding). These graphs reaffirm that the proposed *eeAlgorithm* betters the results obtained with the *optimal-IBI* scheme. It is observed that the

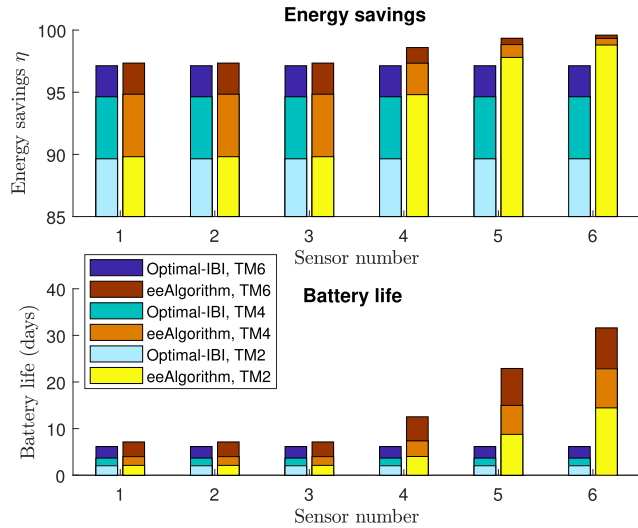


FIGURE 10. Energy savings and battery lifespan with varying number of repetitions.

energy savings and battery duration are reduced as N_{REPI} increases. The reason is that a higher N_{REPI} value means longer packets need to be transmitted and, consequently, more energy is required. The obtained T_{IBI} value is 100 ms with *optimal-IBI*, independently of the number of repetitions. The explanation is that with this proposal $T_{IBI} = GCD\{Tg_i, i = 1, 2, \dots, N\}$ and, thus, it does not depend on the packets size. On the contrary, with the *eeAlgorithm*, T_{IBI} values are 2000 ms, 1000 ms and 400 ms for $N_{REPI} = \{1, 2, 4\}$, respectively. The degree of improvement achieved with the present proposal in comparison to [5] increases with the number of repetitions (a nearly 515%, 620% and 710% rise is attained for sensor 6 with $N_{REPI} = \{1, 2, 4\}$, respectively).

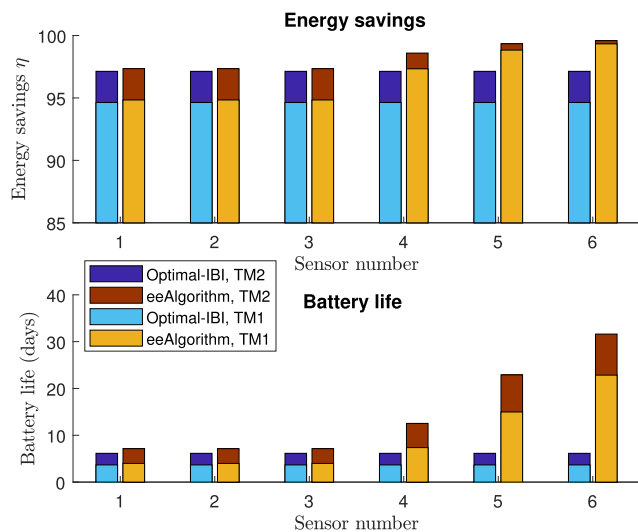


FIGURE 11. Energy savings and battery lifetime with and without BCH.

Fig. 11 represents the energy savings and battery lifetime when TM1 and TM2 are used (with and without BCH coding, respectively, and 4 repetitions), for a MAC frame body length $L_f = 50$ bytes (with a shorter L_f the additional parity bits

TABLE 4. Scenarios corresponding to Figs. 12 and 13.

Sensor number	1	2	3	4	5	6	7
Tg_i [ms]	100	100	200	250	500	750	1000
received SNR [dB]							
with $L_f = 50$ bytes	3	4	6	7	9	11	-
with $L_f = 200$ bytes	3	4	6	7.5	9	11	-
with $L_f = 500$ bytes	3	5	6	8	9	11	-
Selected TM	1	2	3	4	5	6	-

have a higher relative weight and, consequently, the effects of BCH coding can be easily demonstrated). The *optimal-IBI* is $T_{IBI} = 100$ ms with both TMs, whereas with the *eeAlgorithm* $T_{IBI} = 1000$ ms with TM1 and $T_{IBI} = 2000$ ms with TM2. It leads to an increase in energy consumption when BCH coding is applied to the MPDU, as a result of the higher number of bits to be transmitted. It can be observed that the *eeAlgorithm* achieves a better performance than the *optimal-IBI* proposal, particularly for sensors with longer data transmission periods (approximately 600% and 500% increase for sensor 6 with and without BCH, respectively).

C. TRANSMISSION MODE SELECTION ALGORITHM RESULTS ANALYSIS

The dependence of the proposed TM selection algorithm on the received SNR as well as on P_0 has been studied considering a SmartBAN consisting of seven sensors with the characteristics summarized in Table 4, with a target PER $P_0 = 10^{-2}$ for sensors numbered from one to six. Results have been computed for different MAC frame body lengths, $L_f = 50$ bytes, 200 bytes and 500 bytes. As it can be observed, the SNR values have been set in order to force each sensor in the studied SmartBAN to select a different TM. Sensor number seven is the one whose behavior is the target of this analysis. Two different Case Studies have been considered. In the First one, sensor number seven has a target PER $P_0 = 10^{-2}$ and is analyzed under received SNR values ranging from 0 dB to 12 dB. In the Second Case Study, the target sensor experiences an $E_b/N_0 = 7$ dB with varying values of P_0 from 10^{-8} to 1.

Fig. 12 depicts results corresponding to the First Case Study. From the shape of this plot one can infer that a greater average received SNR, corresponding to a better channel quality, results in the growth of battery lifespan. This behavior stems from the fact that, as already summarized in table 2, higher order TMs correspond to less robust transmission schemes that, as a consequence, lead to higher transmission rates. Moreover, the resource allocation scheme presented in Section IV has been designed with the objective of maximizing the data rate while maintaining the instantaneous PER below a prescribed value P_0 . Therefore, greater average received SNR values result in the use of higher order TMs, which achieve faster average transmission rates and, consequently, longer battery durations. On the contrary, longer MAC frame body lengths lead to higher PER values and, therefore, require the use of more robust (lower order) TMs to fulfill the prescribed P_0 which, as a consequence, decrease the battery lifetime. It is worth noting

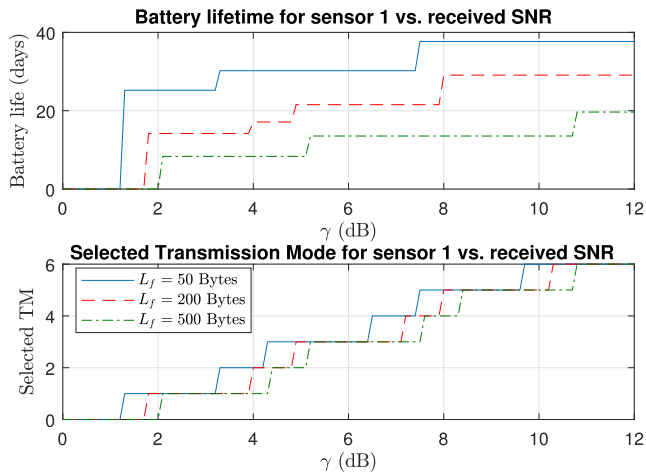


FIGURE 12. Battery lifetime and selected TM for sensor 1 in SmartBAN with 7 on-body sensors vs. received SNR.

that a longer MAC frame body length requires better channel conditions to select a given TM.

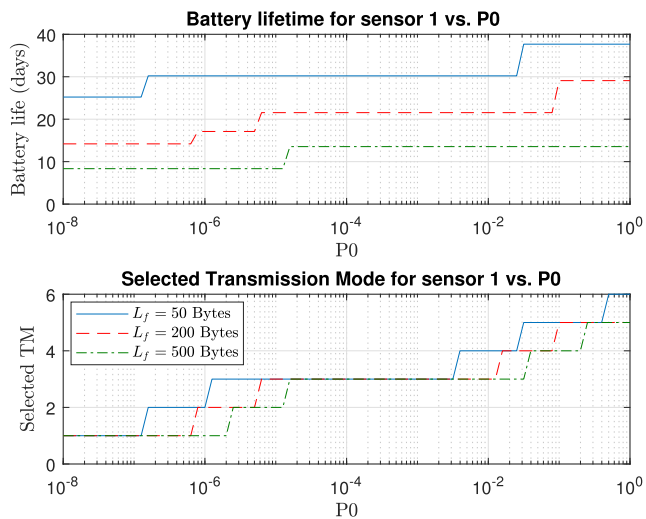


FIGURE 13. Battery lifetime and selected TM for sensor 1 in SmartBAN with 7 on-body sensors vs. P_0 .

Concerning the *Second Case Study*, Fig. 13 reveals that, as expected, less restrictive requirements of the target PER, that is, an increase of P_0 , implies the utilization of higher order TMs, causing a growth of the service rate and, thus, a longer battery lifespan. Concerning the MAC frame body lengths, similarly to what has been already deduced in *Case Study 1*, longer L_f values involve the selection of lower order TMs, increasing transceivers energy consumption. It can also be inferred that a longer L_f value requires higher P_0 values to select a given TM.

VII. CONCLUSION AND FUTURE WORK

In this paper, an energy-efficient resource allocation algorithm for periodic monitoring in SmartBANs has been developed. Furthermore, a link adaptation scheme that selects

the TM to be used at the PHY layer while maintaining the instantaneous PER below a target value, has also been proposed. Bearing the minimization of energy consumption in mind, the presented *eeAlgorithm* has the ability to group several data generation periods of sensors in order to derive the longest possible T_{IBI} that satisfies the emergency and scheduled traffic delay requirements. Mathematical formulas for delay, energy savings of sensors and hub, and battery lifespan, have been presented.

The proposed framework performance has been analyzed through computer simulation. Numerical examples have demonstrated that the undesirable effects of the channel impairments can be effectively mitigated using the presented TM selection algorithm, by adapting the SmartBAN PHY layer adjustable parameters to the channel characteristics, i.e. the use or not of BCH coding for the MPDU and the possibility of PPDU repetition. Results have shown that higher order TMs, which correspond to faster transmission rates but less robust transmission schemes, are selected for better channel conditions, leading to higher energy efficiency and, consequently, longer battery lifetimes. Besides, the effectiveness of this proposal has been contrasted with the work presented in [5], proving that the *eeAlgorithm* achieves a noticeable improvement on energy efficiency and battery duration, specially for sensors with long data generation periods. This behavior stems from the fact that these sensors transceivers can remain longer in sleep mode by means of grouping several consecutive transmissions to be jointly delivered to the hub afterwards.

The scenario that has been analyzed in this research work corresponds to a specific snapshot of a given WBAN, with sensors and hub holding still at their positions for that particular time instant. Nevertheless, the proposed framework could be applied to analyze how the temporal variations of large-scale and small-scale fading [26], as well as fading correlation, may impact the system behavior in a time-varying scenario. Moreover, and taking into account that the wireless communication module is usually the most power-hungry unit in a wearable system [27], the adoption of simple processing and data compression schemes such as the ones described in [28], [29] constitute another promising avenue for future work. Such techniques could be remarkably effective to further increase the battery lifetime when combined with the grouping of consecutive transmissions of sensors performed by the presented proposal.

REFERENCES

- [1] *IEEE Standard for Local and Metropolitan Area Networks—Part 15.6: Wireless Body Area Networks*, Standard 802.15.6, 2012.
- [2] *ETSI Smart Body Area Network (SmartBAN)—Enhanced Ultra-Low Power Physical Layer*, document ETSI TS 103 326 v1.1.1, 2015.
- [3] *ETSI Smart Body Area Network (SmartBAN)—Low Complexity Medium Access Control (MAC) for SmartBAN*, document ETSI TS 103 325 v1.1.1, 2015.
- [4] R. Matsuo, T. Nabetani, H. Tanakay, W. H. Chin, and S. Subramani, “Performance of simple and smart PHY/MAC mechanisms for body area networks,” in *Proc. IEEE Int. Conf. Commun. (ICC)*, London, U.K., Jun. 2015, pp. 501–506.

- [5] L. Ruan, M. P. I. Dias, and E. Wong, "SmartBAN with periodic monitoring traffic: A performance study on low delay and high energy efficiency," *IEEE J. Biomed. Health Inform.*, vol. 22, no. 2, pp. 471–482, Mar. 2018.
- [6] B. Johnny and A. Anpalagan, "Body area sensor networks: Requirements, operations, and challenges," *IEEE Potentials*, vol. 33, no. 2, pp. 21–25, Mar. 2014.
- [7] Z. Liu, B. Liu, C. Chen, and C. W. Chen, "Energy-efficient resource allocation with QoS support in wireless body area networks," in *Proc. IEEE Global Commun. Conf. (GLOBECOM)*, San Diego, CA, USA, Dec. 2015, pp. 1–6.
- [8] B. Liu, Z. Yan, and C. W. Chen, "Medium access control for wireless body area networks with QoS provisioning and energy efficient design," *IEEE Trans. Mobile Comput.*, vol. 16, no. 2, pp. 422–434, Feb. 2017.
- [9] N. F. Timmons and W. G. Scanlon, "An adaptive energy efficient MAC protocol for the medical body area networks," in *Proc. Wireless VITAE Aalborg*, Denmark, 2009, pp. 587–593.
- [10] G. Fang and E. Dutkiewicz, "BodyMAC: Energy efficient TDMA-based MAC protocol for Wireless Body Area Networks," in *Proc. 9th Int. Symp. Commun. Inf. Technol.*, Icheon-si, South Korea, Sep. 2009, pp. 1455–1459.
- [11] J. Ramis-Bibiloni and L. Carrasco-Martorell, "An energy-efficient and delay-constrained resource allocation scheme for periodical monitoring traffic in SmartBANs," in *Proc. IEEE Biomed. Circuits Syst. Conf. (BioCAS)*, Turin, Italy, Oct. 2017, 2017, pp. 1–4.
- [12] A. Goldsmith, *Wireless Communications*. 1st ed. Cambridge, U.K.: Cambridge Univ. Press, 2005.
- [13] R. T. Caldeira and G. G. Neto, *Long Term Evolution. Telecommunications and Information Technology (Link Adaptation LTE Systems)*, A. Paradisi, M. Yacoub, F. L. Figueiredo, and T. Tronco, Eds. Cham, Switzerland: Springer, 2016.
- [14] M. Barbi, K. Sayrafian, and M. Alasti, "Application of link adaptation in body area networks," in *Proc. IEEE 28th Annu. Int. Symp. Pers., Indoor, Mobile Radio Commun. (PIMRC)*, Montreal, QC, Canada, Oct. 2017, pp. 1–6.
- [15] F. Martelli, R. Verdona, and C. Buratti, "Link adaptation in wireless body area networks," in *Proc. IEEE 73rd Veh. Technol. Conf. (VTC)*, Yokohama, Japan, May 2011, pp. 1–5.
- [16] Q. Liu, S. Zhou, and G. Giannakis, "Cross-layer combining of adaptive modulation and coding with truncated ARQ over wireless links," *IEEE Trans. Wireless Commun.*, vol. 3, no. 5, pp. 1746–1755, Sep. 2004.
- [17] Q. Liu, S. Zhou, and G. Giannakis, "Queuing with adaptive modulation and coding over wireless links: Cross-Layer analysis and design," *IEEE Trans. Wireless Commun.*, vol. 4, no. 3, pp. 1142–1153, May 2005.
- [18] D. Niyato and E. Hossain, "Queuing with adaptive modulation and coding over wireless links: Cross-Layer analysis and design," *IEEE Trans. Mobile Comput.*, vol. 6, no. 3, pp. 322–335, Mar. 2007.
- [19] J. Ramis and G. Femenias, "Cross-layer design of adaptive multirate wireless networks using truncated HARQ," *IEEE Trans. Veh. Technol.*, vol. 60, no. 3, pp. 944–954, Mar. 2011.
- [20] L. Hanlen, V. Chaganti, B. Gilbert, D. Rodda, T. Lamaheva, and D. Smith, "Open-source testbed for Body Area Networks: 200 sample/sec, 12 hrs continuous measurement," in *Proc. IEEE 21st Int. Symp. Pers., Indoor Mobile Radio Commun. Workshops*, Istanbul, Turkey, Sep. 2010, pp. 66–71.
- [21] A. Vakili, M. Sharif, and B. Hassibi, "The Effect of channel estimation error on the throughput of broadcast channels," in *Proc. IEEE Int. Conf. Acoust. Speed Signal Process. Proc.*, Toulouse, France, Aug. 2006, pp. 29–32.
- [22] G. Oien, H. Holm, and K. Hole, "Impact of channel prediction on adaptive coded modulation performance in Rayleigh fading," *IEEE Trans. Veh. Technol.*, vol. 53, no. 3, pp. 758–769, May 2004.
- [23] *IEEE Draft Health Informatics—Point-of-Care Medical Device Communication—Technical Report—Guidelines for the use of RF wireless technology*, Standard P11073-00101/D5, Jun. 2008.
- [24] *MATLAB Release 2017a*, The MathWorks, Natick, MA, USA, 2017.
- [25] N. Cordeschi, D. Amendola, M. Shojafar, and E. Baccarelli, "Distributed and adaptive resource management in Cloud-assisted Cognitive Radio Vehicular Networks with hard reliability guarantees," *Veh. Commun.*, vol. 2, no. 1, pp. 1–12, Jan. 2015.
- [26] K. Y. Yazdandoost, *Channel Model for Body Area Network (BAN)*, Standard IEEE P802.15-08-0780-12-0006, IEEE P802.15 Working Group for Wireless Personal Area Networks, (WPANs) 2010.
- [27] E. Nemat, M. Deen, and T. Mondal, "A wireless wearable ECG sensor for long-term applications," *IEEE Commun. Mag.*, vol. 50, no. 1, pp. 36–43, Jan. 2012.
- [28] A. Watkins, V. N. Mudhiredy, H. Wang, and S. Tragoudas, "Adaptive compressive sensing for low power wireless sensors," in *Proc. 24th Great Lakes Symp. VLSI*, Houston, TX, USA, 2014, pp. 99–104.
- [29] A. Ukil, S. Bandyopadhyay, and A. Pal, "IoT data compression: Sensor-agnostic approach," in *Proc. Data Compress. Conf.*, Snowbird, UT, USA, Apr. 2015, pp. 303–312.



JAUME RAMIS-BIBILONI (Member, IEEE) was born in Sencelles, The Balearic Islands, Spain, in 1972. He received the Engineer of Telecommunication degree from the Polytechnic University of Catalonia, in 1997, and the Ph.D. degree in computer science from the University of the Balearic Islands (UIB), Spain, in 2012. Since 2002, he has held several positions at the Department of Mathematics and Informatics, UIB, where he is currently an Associate Professor. His current research interests are wireless personal communication systems, with particular emphasis on wireless body area networks. He is the author of articles in international journals on this topic as well as of communications to international conferences. He has been involved in projects concerned with Wireless LAN (WLAN) design, funded by the Spanish and Balearic Islands governments (MARIMBA, XISPES, COSMOS, AM3DIO, ELISA, and TERESA). Dr. Ramis-Bibiloni was a co-recipient of the Best Paper Award at the IEEE Vehicular Technology Conference 2009-Spring.



LOREN CARRASCO-MARTORELL was born in Puigpunyent, The Balearic Islands, Spain, in 1968. She received the Engineer degree in telecommunication from the Polytechnic University of Catalonia, in 1992, and the Ph.D. degree in computer science from the University of the Balearic Islands (UIB), Spain, in 2005. Since 1998, she has held several positions at the Department of Mathematics and Informatics, UIB, where she is currently an Associate Professor and the Dean of the Engineering and Mathematics Faculty. Her current research interests are wireless personal communication systems, with particular emphasis on wireless body area networks. She is the author of articles in international journals on this topic as well as of communications to international conferences. She has been involved in national and international projects concerned with Wireless networks design, funded by the European, the Spanish and Balearic Islands governments (CODIT, MONET, MARIMBA, XISPES, COSMOS, AM3DIO, ELISA, and TERESA). Dr. Carrasco-Martorell was a co-recipient of the Best Paper Award at the IEEE Vehicular Technology Conference 2009-Spring.

• • •